Airborne LiDAR System (ALS) Ranging and Georeferencing

ROD PICKENS
CHIEF SCIENTIST, CNS
SIERRA NEVADA CORPORATION

FRIDAY MARCH 31, 2017

Topics to cover

- Remote Sensing with LiDAR
- Airborne LiDAR Systems
- Ranging methods for full-waveform LiDAR
- Georeferencing LiDAR point cloud
- Conclusion
- Referencess

Remote Sensing with LiDAR

LiDAR data

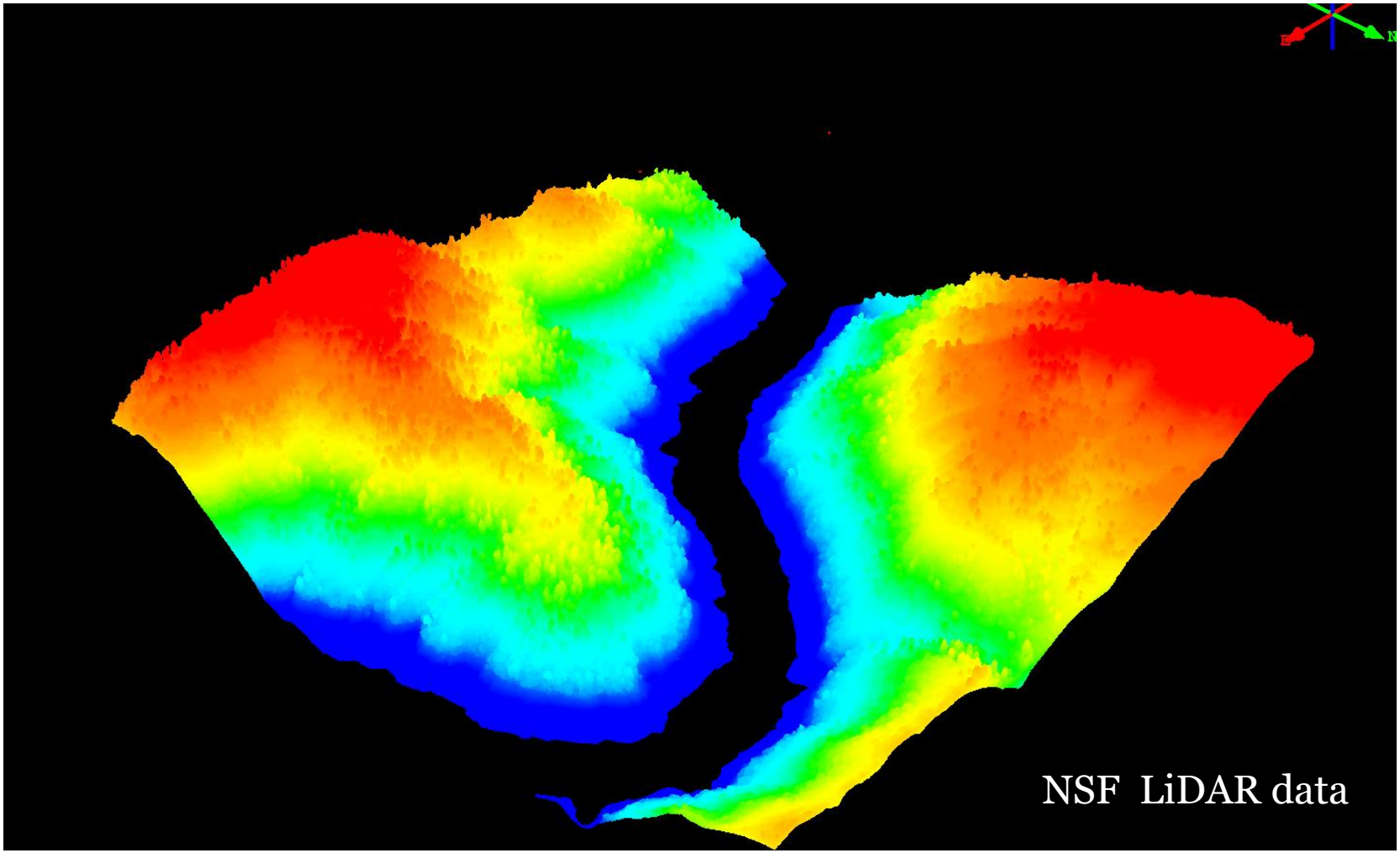

Airborne LiDAR System: Overview

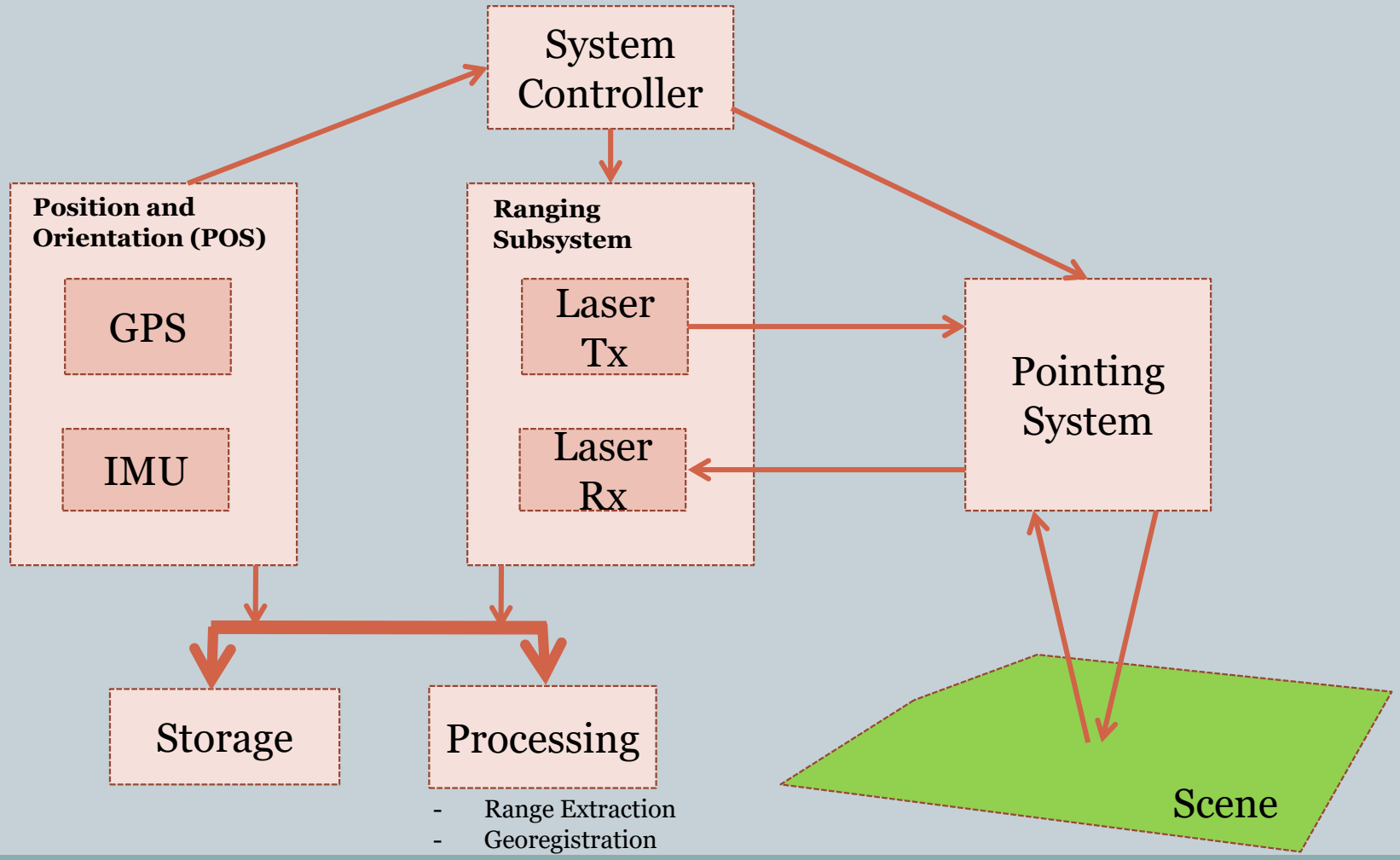

*NGA.SIG.0004

Pointing

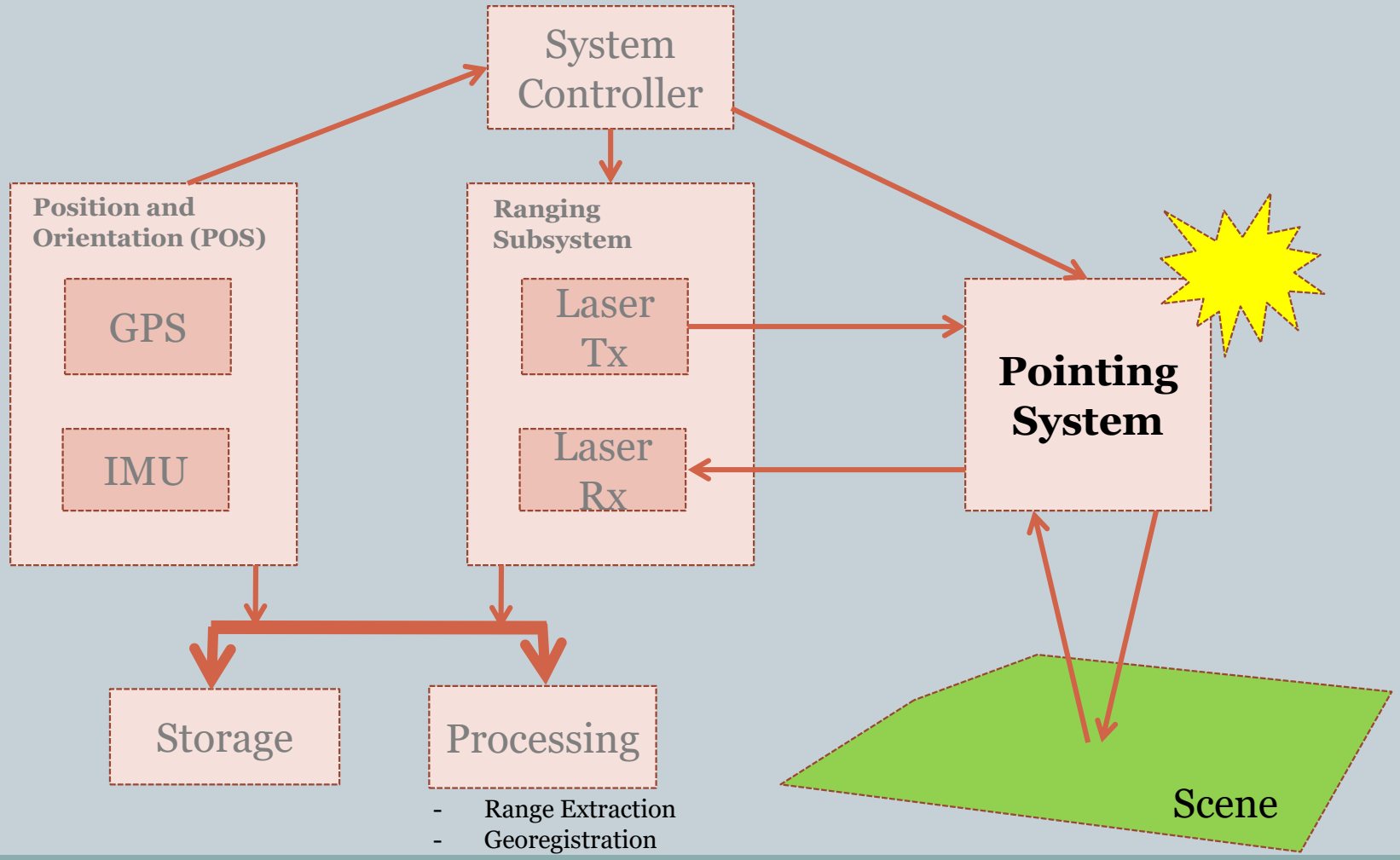

*NGA.SIG.0004

LiDAR Pointing Mechanisms

LiDAR

Scanner:
Flying Spot

Scannerless:
Time-of-Flight Camera

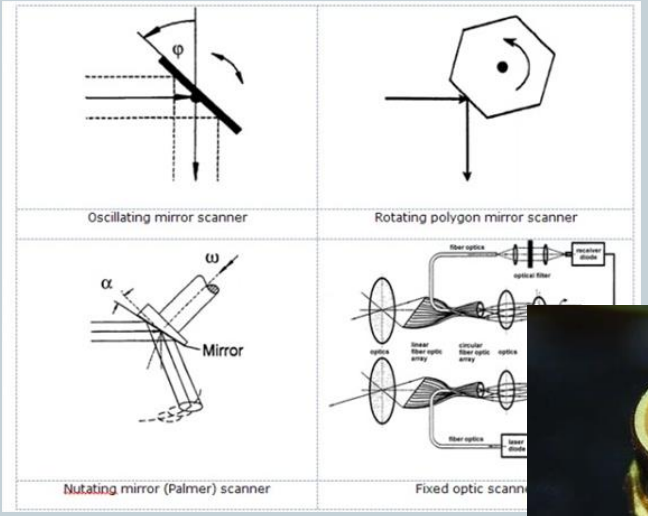

Avalanche Photo Diode:
Photo by Radovan Blazek

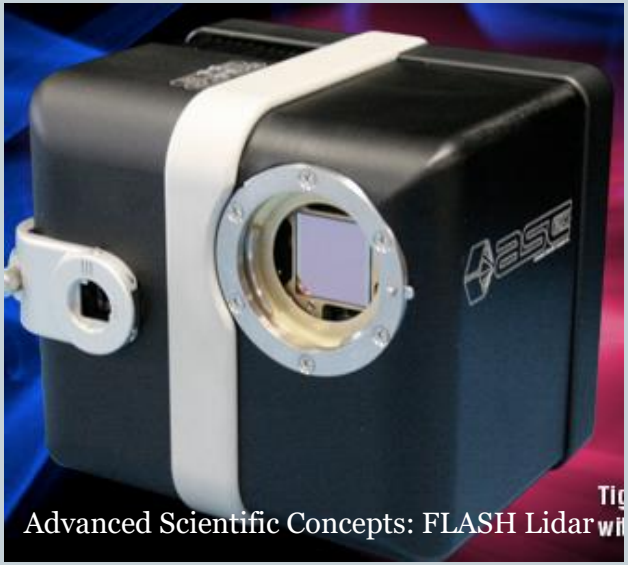

Advanced Scientific Concepts: FLASH Lidar

Range Extraction

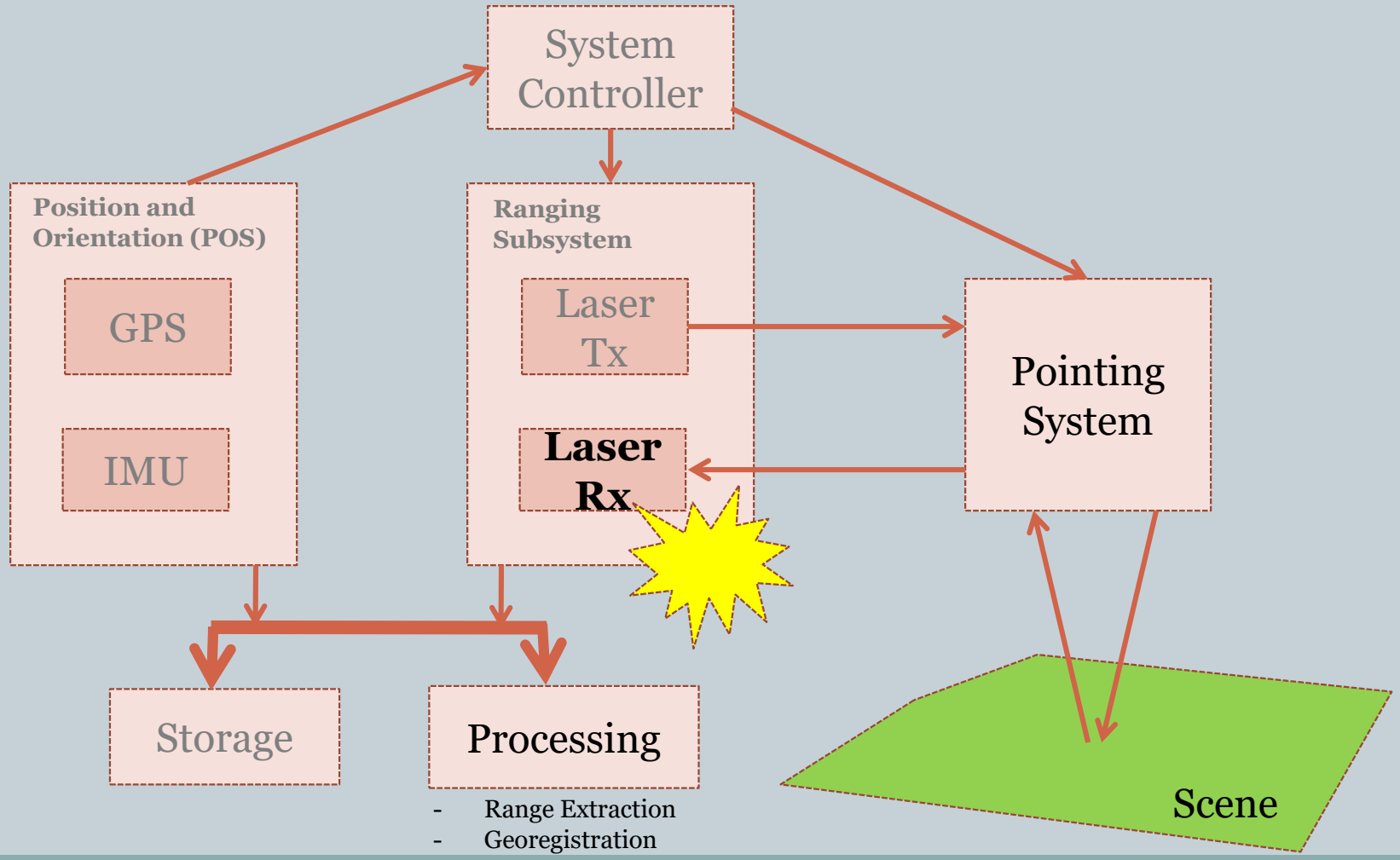

*NGA.SIG.0004

Approaches to Range Extraction

Discrete returns
(hardware based)

Full-waveform returns
(software based)

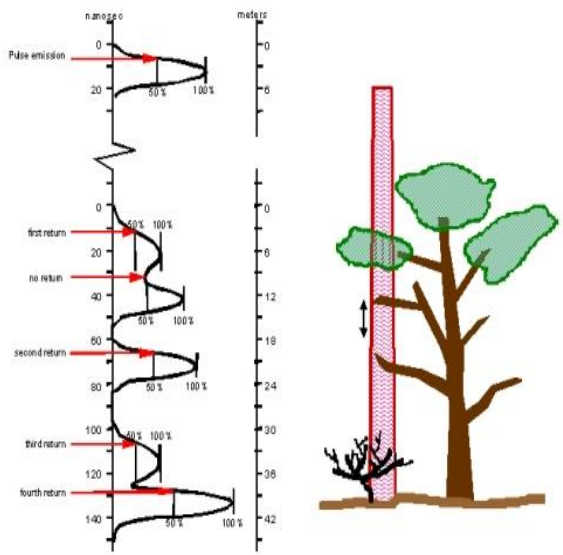

Figure 1.05: Multiple lidar returns can be generated from a single emitted pulse. Depending on the detection capabilities of the lidar sensor, two or more of these returns may be recorded as data points.

SOURCE: ASPRS

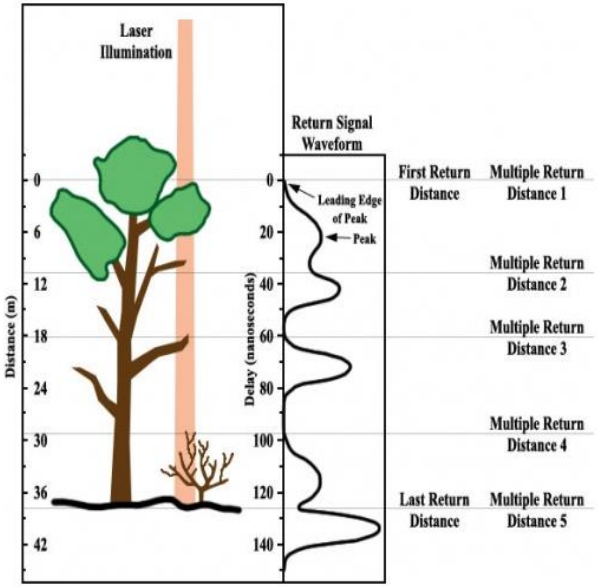

Figure 1.07: In a waveform lidar, the entire return pulse is digitized and recorded. In a discrete multiple-return lidar, only the peaks would be recorded.

SOURCE: ASPRS

Time-of-Flight Imaging

Principles of ToF Imaging

Pulsed Modulation

- Measure distance to a 3D object by measuring the absolute time a light pulse needs to travel from a source into the 3D scene and back, after reflection
- Speed of light is constant and known, $c = 3 \cdot 10^8 m/s$

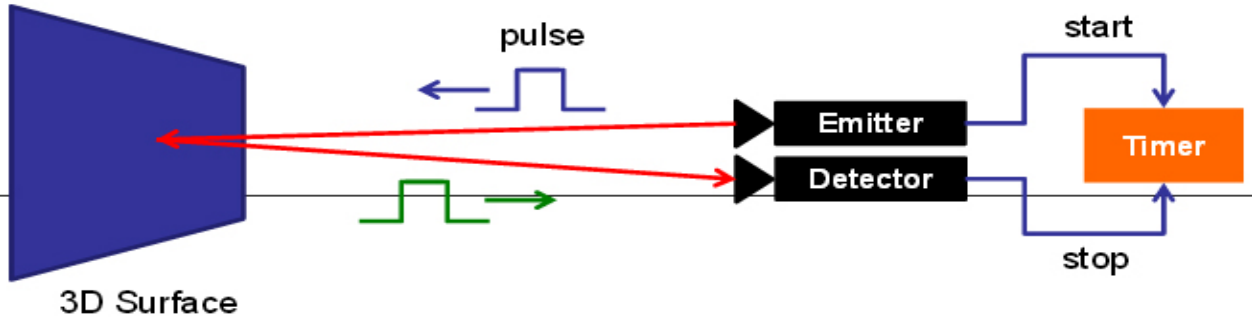

Processing

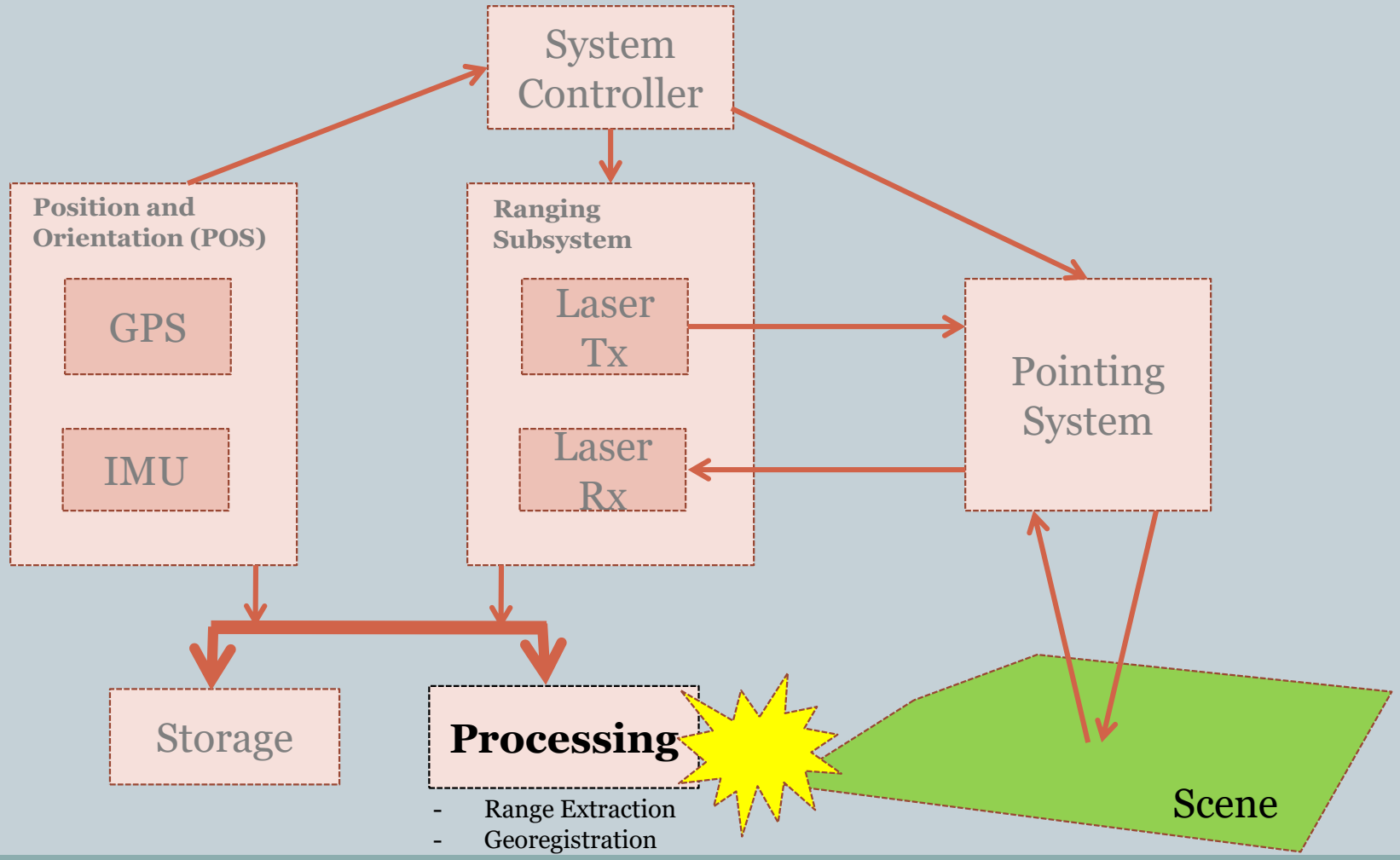

*NGA.SIG.0004

Full-waveform Range Extraction

Full-waveform Range Extraction

Discrete returns
(hardware based)

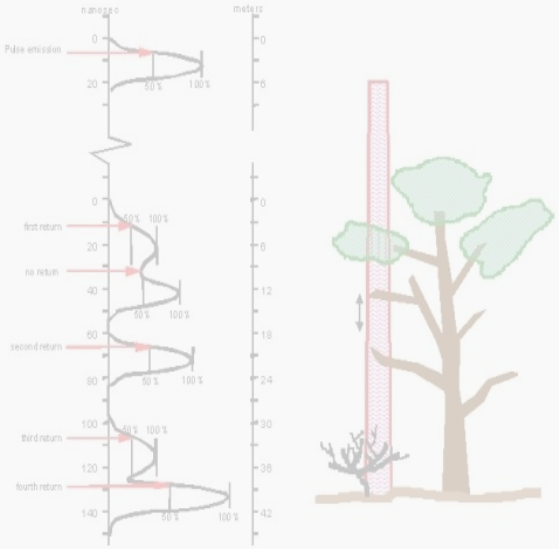

Figure 1.05: Multiple lidar returns can be generated from a single emitted pulse. Depending on the detection capabilities of the lidar sensor, two or more of these returns may be recorded as data points.

SOURCE: ASPRS

Full-waveform returns
(software based)

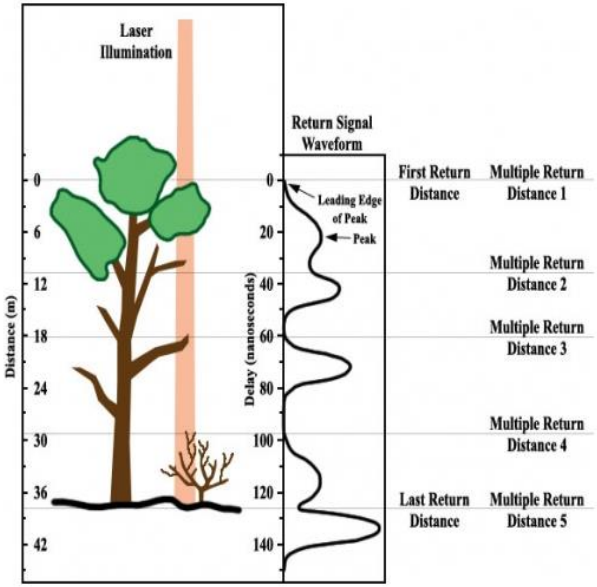

Figure 1.07: In a waveform lidar, the entire return pulse is digitized and recorded. In a discrete multiple-return lidar, only the peaks would be recorded.

SOURCE: ASPRS

Some Methods of Range Extraction

- Gaussian Decomposition
  - Hofton et al. 2000, Persson et al. 2005, …
- Expectation-Maximization Deconvolution
  - Parrish et al 2007, Figueiredo and Nowak 2003
- Wiener Deconvolution and Decomposition
  - Jutzi and Silla 2006

- Other methods
  - Matched filtering
  - B-Splines Approach
    - Roncat et al. 2010
  - Average Square Difference Function
    - Wagner et al 2007

Gaussian Decomposition

Gaussian Decomposition

Each LiDAR waveform is a linear combination of Gaussian components.

Figure 2 Gaussian decomposition of the LMS-Q560 waveform showing the recorded waveform (points), the Gaussian functions for all four detected echoes (broken lines), and the overall fitted model (solid line). The model parameters of the individual echo pulses are given in table 2.

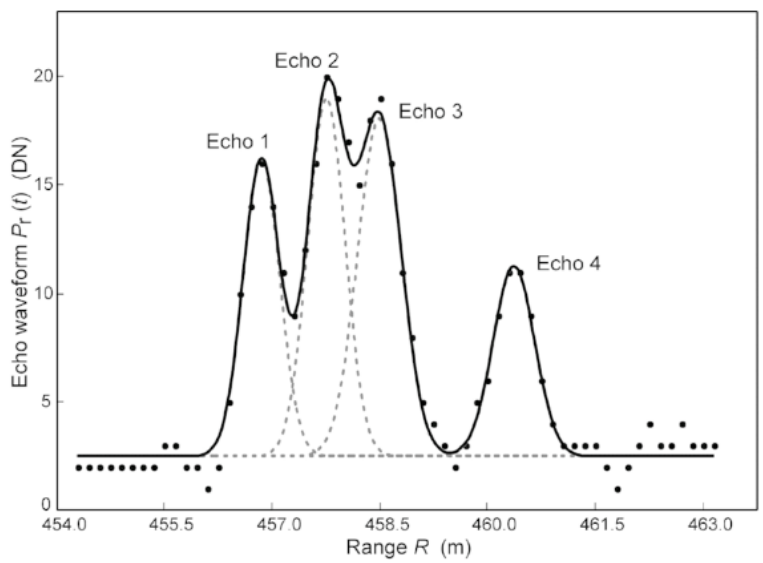

$$\hat{y}(t) = \sum_{i=1}^{N} \alpha_i exp\left\{-\frac{1}{2\sigma_i^2}(t-\mu_i)^2\right\}$$

$$\alpha_i = amplitude\ of\ ith\ component$$
$$\sigma_i = width\ of\ ith\ component$$
$$\mu_i = \text{position of ith component}$$

Sources: References 4 and 5

Functional Diagram of Gaussian Decomposition

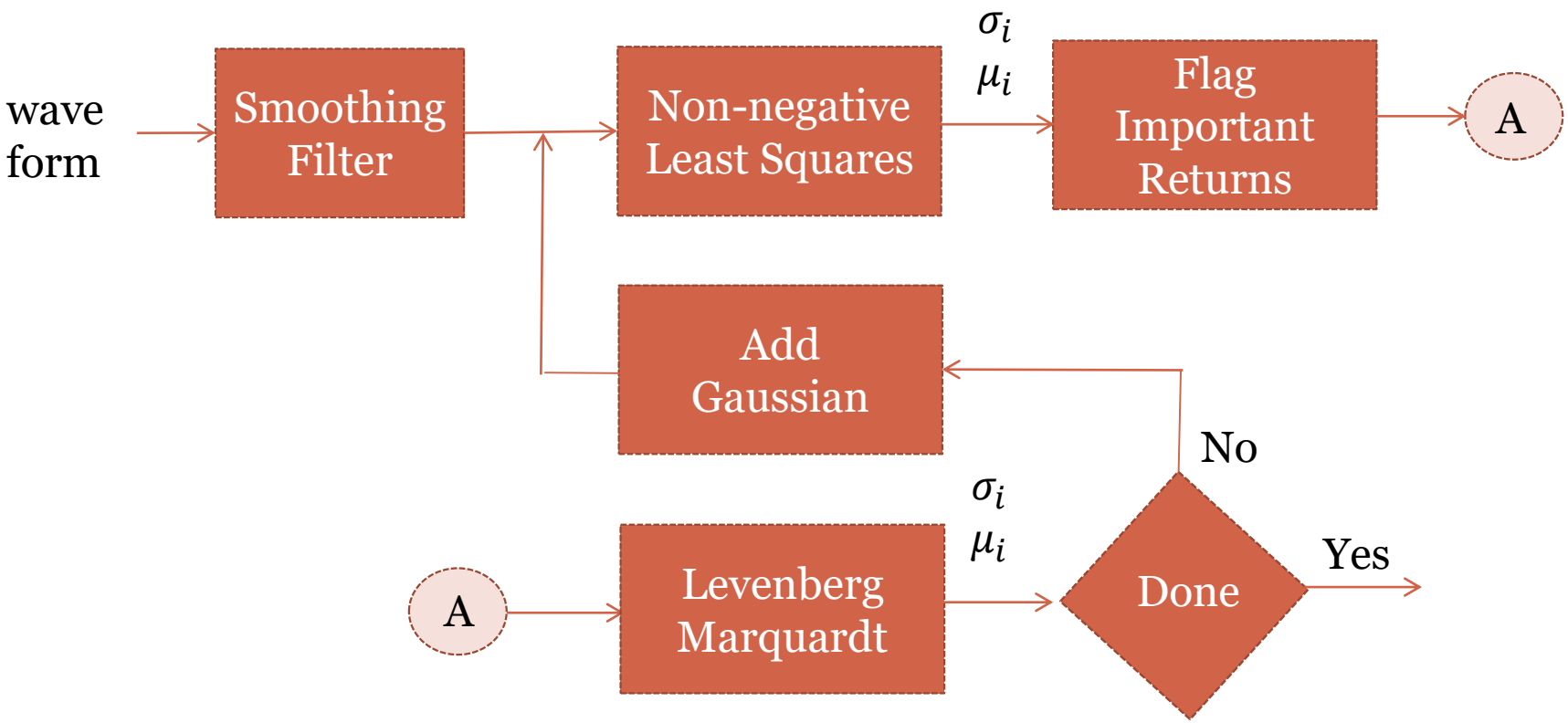

Hofton: Reference 3 and 4

Expectation Maximization Deconvolution

Deconvolution: Determine x[n]

Given ***input*** $\boldsymbol{y[n]}$ *which is the received full waveform:*

$$y[n] = h[n] * x[n] + \eta[n]$$

where

$\boldsymbol{x[n]}$ **is the full waveform representation of scene**

$h[n]$ is system impulse response (optics, electronics, atmosphere)

$\eta[n]$ is white Gaussian noise

estimate via deconvolution

$$\boldsymbol{x[n]}$$

which is the signal of interest.

Expectation Maximization (1/5)

Maximum Likelihood

$$\hat{\theta} = \underset{\theta}{\operatorname{argmax}} \left[\sum_{i=1}^{I} log[\underbrace{\Pr(x_i|\theta)}] \right]$$

Expectation maximization
(hidden variables h_i)

$$\hat{\theta} = \underset{\theta}{\operatorname{argmax}} \left[\sum_{i=1}^{I} log \left[\underbrace{\int \Pr(x_i, h_i|\theta)\, dh_i} \right] \right]$$

$$\Pr(x_i|\theta) = \int \Pr(x_i, h_i|\theta)\, dh_i$$

EM and Full-waveform (2/5)

Apply EM to
Mixture of Gaussians

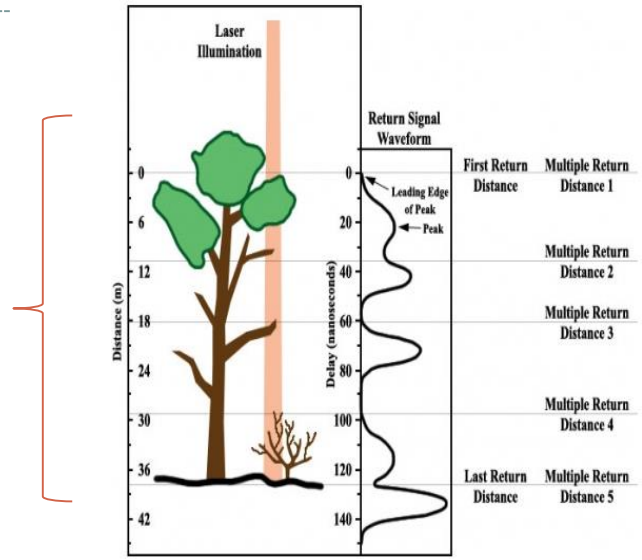

Figure 1.07: In a waveform lidar, the entire return pulse is digitized and recorded. In a discrete multiple-return lidar, only the peaks would be recorded.

SOURCE: ASPRS

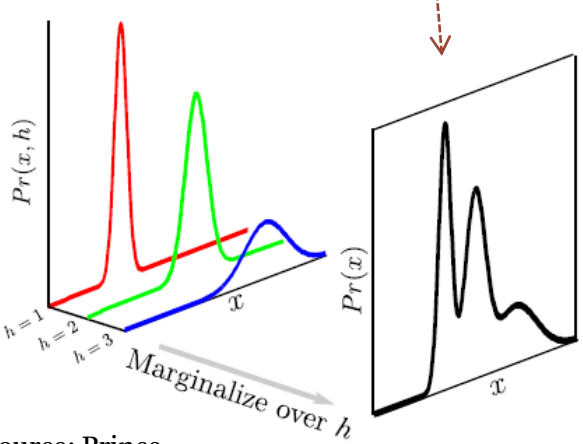

Source: Prince

Figure 7.7 Mixture of Gaussians as a marginalization. The mixture of Gaussians can also be thought of in terms of a joint distribution $Pr(x,h)$ between the observed variable x and a discrete hidden variable h. To create the mixture density we marginalize over h. The hidden variable has a straightforward interpretation: it is the index of the constituent normal distribution.

Expectation Maximization (3/5)

$$\hat{\theta} = \underset{\theta}{\operatorname{argmax}} \underbrace{\left[\sum_{i=1}^{I} log \left[\int \Pr(x_i, h_i | \theta)\, dh_i \right] \right]}_{A}$$

Set a lower bound to the above log likelihood, A, as follows:

$$\sum_{i=1}^{I} q_i(h_i) log \left[\int \frac{\Pr(x_i, h_i | \theta)}{q_i(h_i)} dh_i \right] \leq \underbrace{\sum_{i=1}^{I} log \left[\int \Pr(x_i, h_i | \theta)\, dh_i \right]}_{A}$$

Expectation Maximization (4/5)

Set $q_i(h_i)$ with hidden parameters h_i as follows

E-step: $$q_i(h_i) = P\left(h_i | x_i, \theta^{[t]}\right) = \frac{\Pr\left(x_i \middle| h_i, \theta^{[t]}\right) \Pr(h_i | \theta^{[t]})}{\Pr(x_i)}$$

and maximize for θ as follows

M-step: $$\hat{\theta}^{[t+1]} = \underset{\theta}{\operatorname{argmax}} \sum_{i=1}^{I} q_i(h_i) log \left[\int \Pr\left(x_i, h_i | \hat{\theta}^{[t]}\right) dh_i \right]$$

Range Extraction with EM (5/5)

$$E\ step\text{:}\ \hat{z}^{(t)}[n] = \hat{x}^{(t)}[n] + h[n] * \left(y[n] - h[n] * \hat{x}^{(t)}[n]\right)$$

$$M\ step\text{:}\ \hat{x}^{(t+1)}[n] = \frac{\max\left(\left(\hat{z}^{(t)}[n]\right)^2 - \tau\sigma_\eta^2\right)}{\hat{z}^{(t)}[n]}$$

$\hat{x}^{(t)}[n]$ is estimate of signal at nth iteration
$\hat{z}^{(t)}[n]$ is estimate of missing data

Wiener Deconvolution and Decomposition

Deconvolution

Given ***input*** $\boldsymbol{y[n]}$ *which is the received full waveform:*

$$y[n] = h[n] * x[n] + \eta[n]$$

and

$\boldsymbol{x[n]}$ **is the full waveform representation of scene**
$h[n]$ is system response (optics, electronics, atmosphere)
$\eta[n]$ is white Gaussian noise

estimate via deconvolution

$\boldsymbol{x[n]}$

which is the signal of interest

Wiener Deconvolution

$$y[n] = h[n] * x[n] + \eta[n]$$

$$y[n] = h[n] * x[n]$$

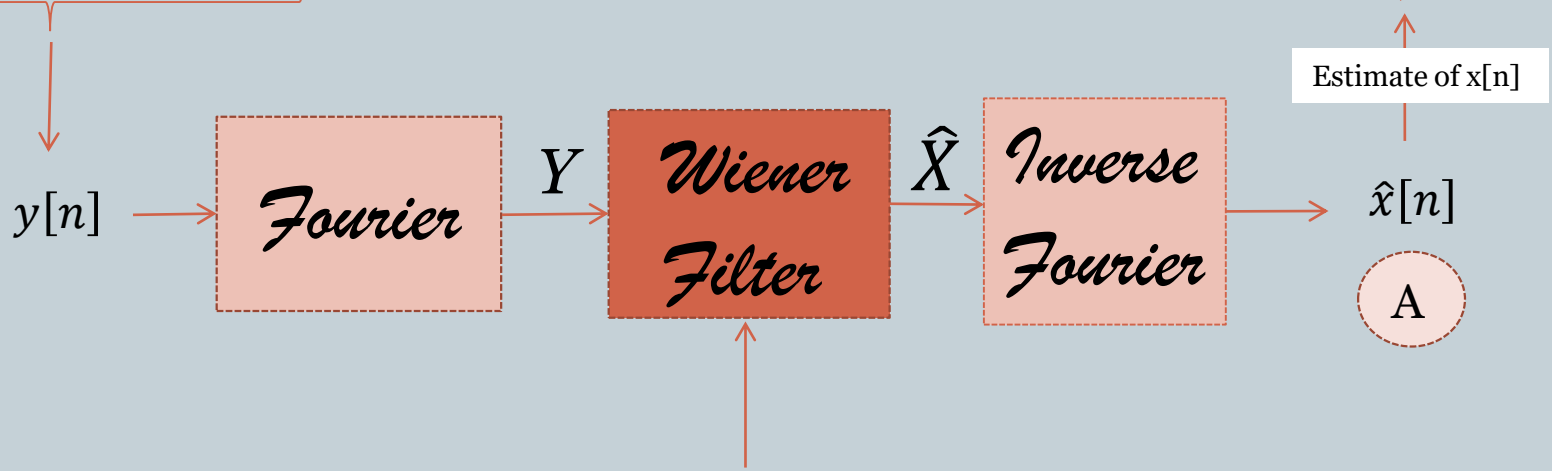

$$\textit{Wiener Filter} = \frac{H^*}{H^* \cdot H + \alpha \cdot NSR}$$

$$NSR \triangleq noise\ to\ signal\ ratio$$

Decomposition

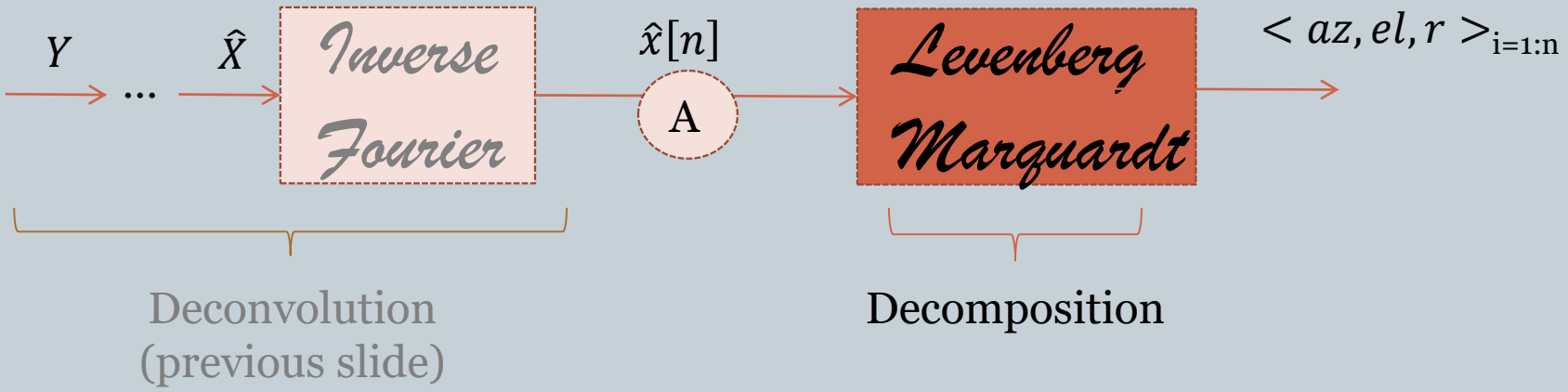

Sensor Coordinates to Georeferenced Coordinates

$<X,Y,Z>_L$

TO

$<LAT,LON,ALT>_{WGS84}$

LiDAR data: Georeferencing

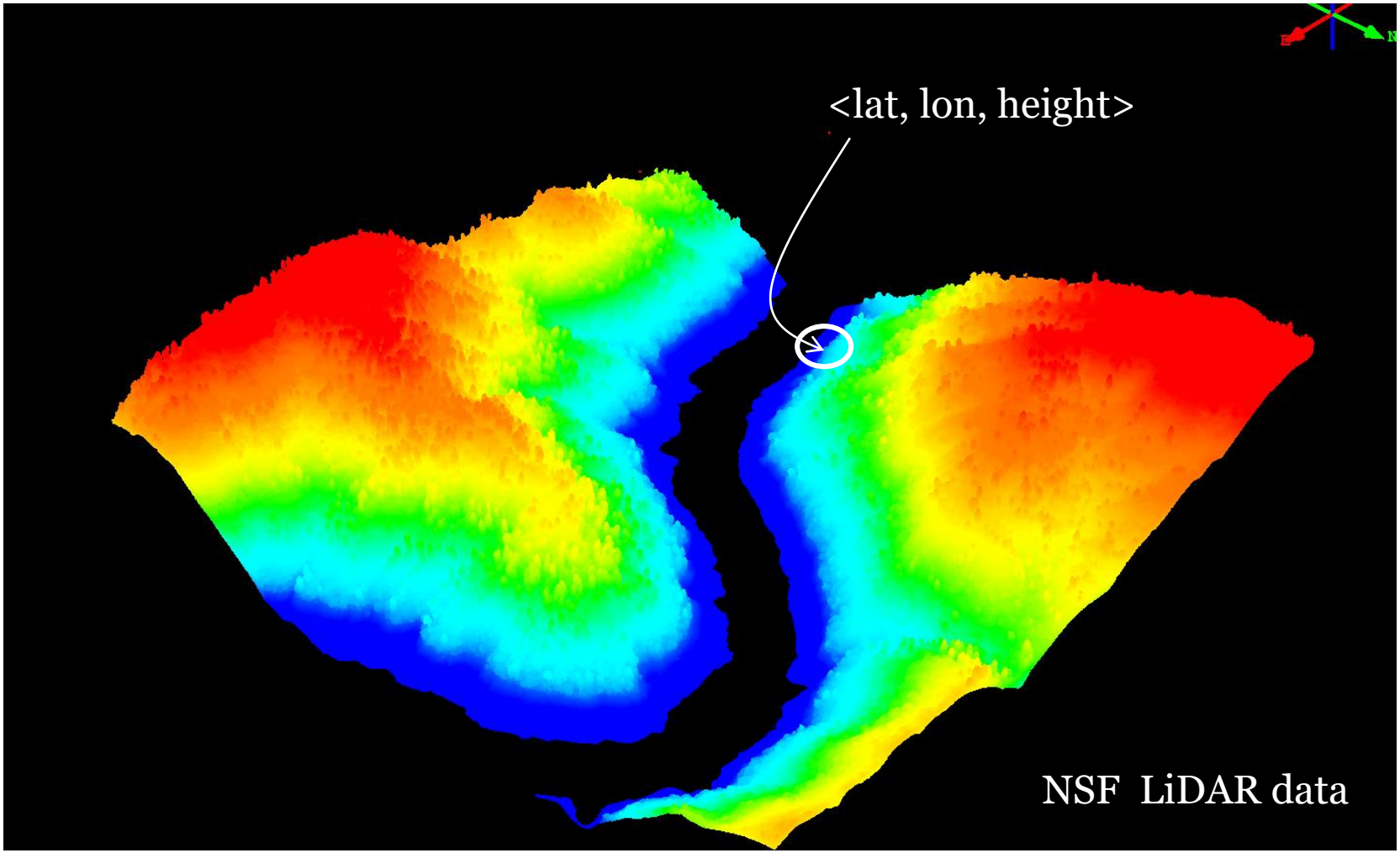

LiDAR data: Georeferencing

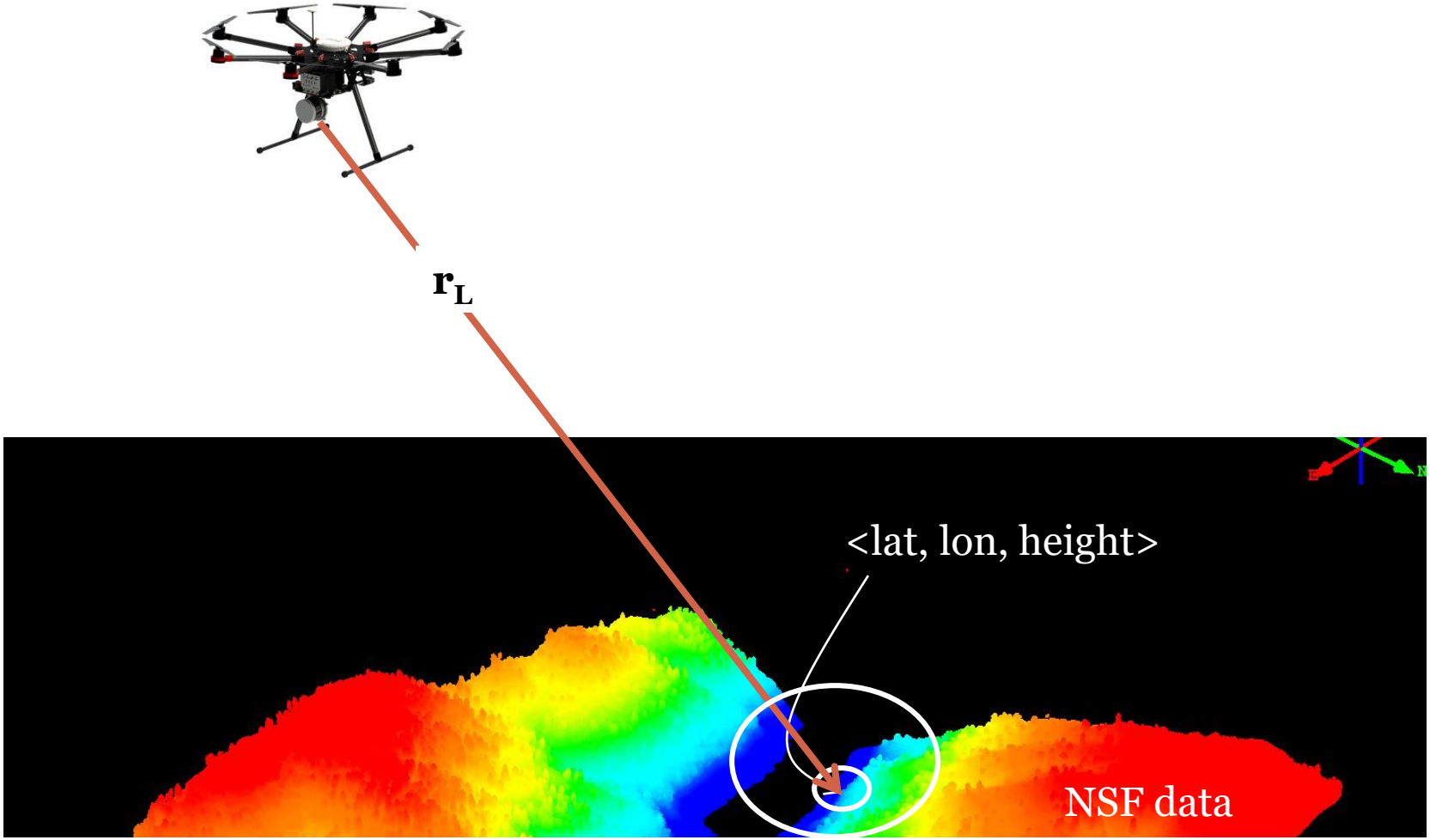

Quadcopter and Geometry

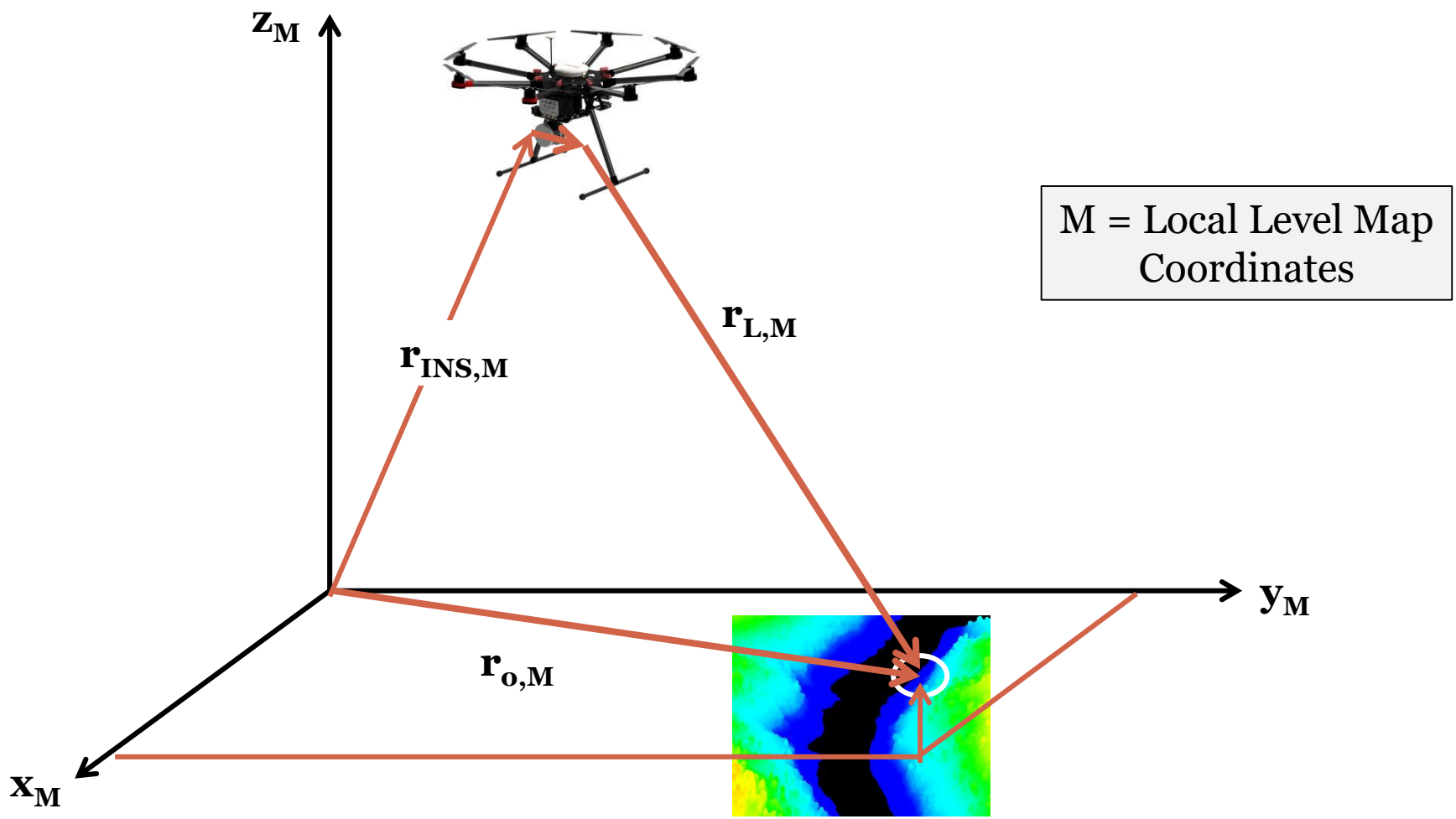

Object in LiDAR Sensor Coordinates

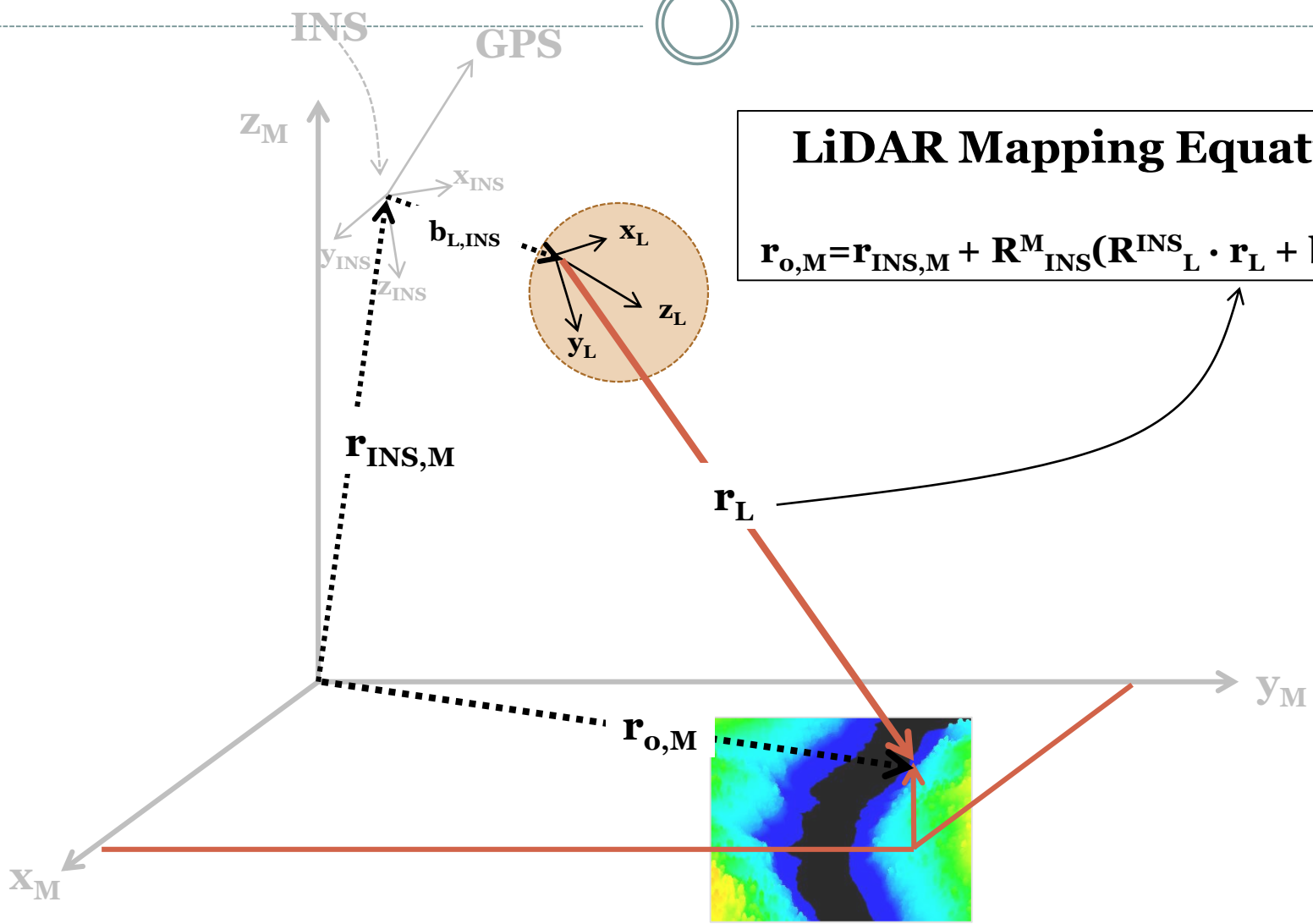

LiDAR Mapping Equation

$$r_{o,M} = r_{INS,M} + R^{M}_{INS}(R^{INS}_{L} \cdot r_L + b_{L,INS})$$

Sensor: Spherical to Cartesian

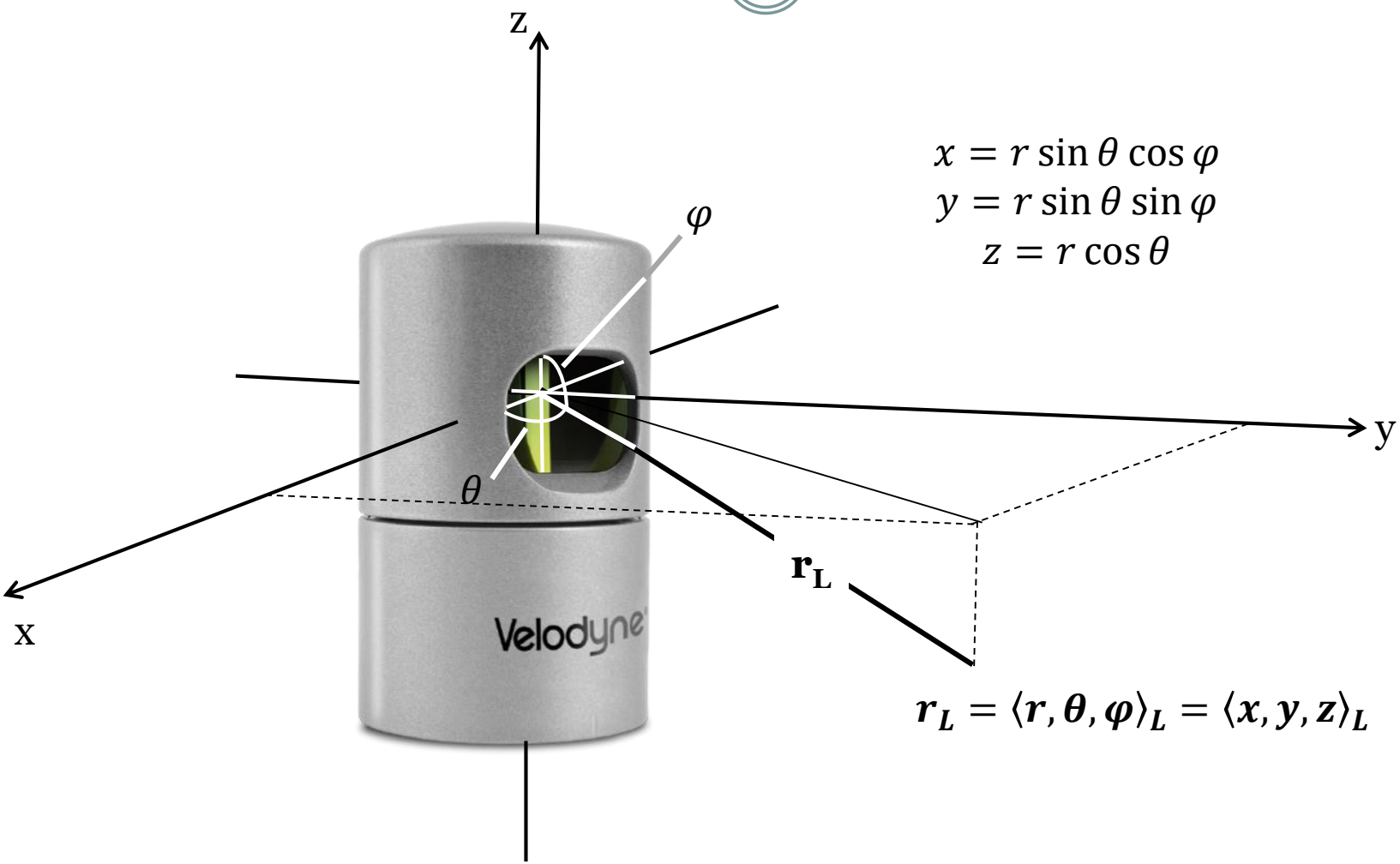

$$x = r \sin\theta \cos\varphi$$
$$y = r \sin\theta \sin\varphi$$
$$z = r \cos\theta$$

$$\boldsymbol{r_L = \langle r, \theta, \varphi \rangle_L = \langle x, y, z \rangle_L}$$

Source: Velodyne Inc.

Object in LiDAR Sensor Coordinates

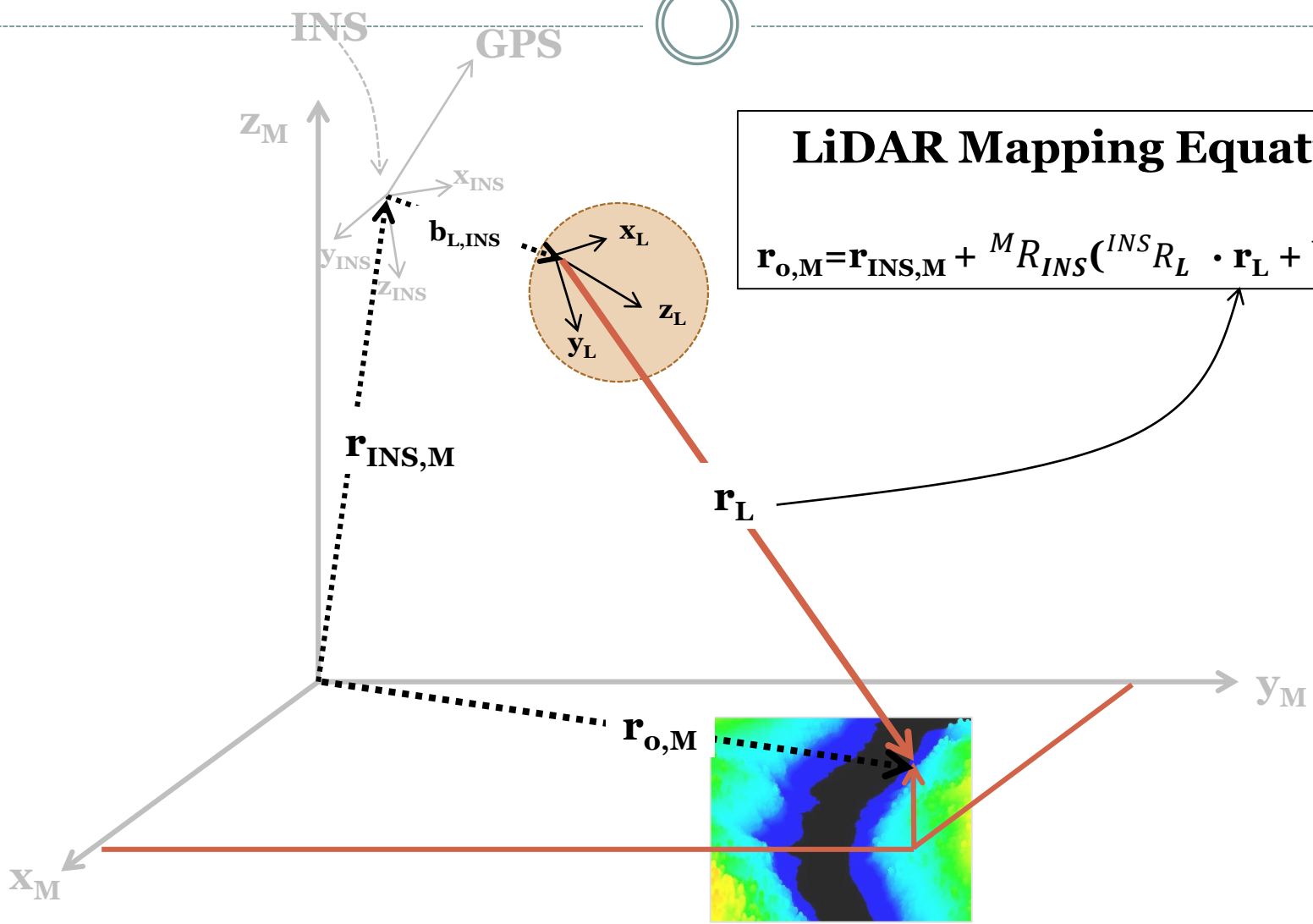

LiDAR Mapping Equation

$$\mathbf{r}_{o,M} = \mathbf{r}_{INS,M} + {}^{M}R_{INS}({}^{INS}R_L \cdot \mathbf{r}_L + \mathbf{b}_{L,INS})$$

Local Level (Map) and ECEF

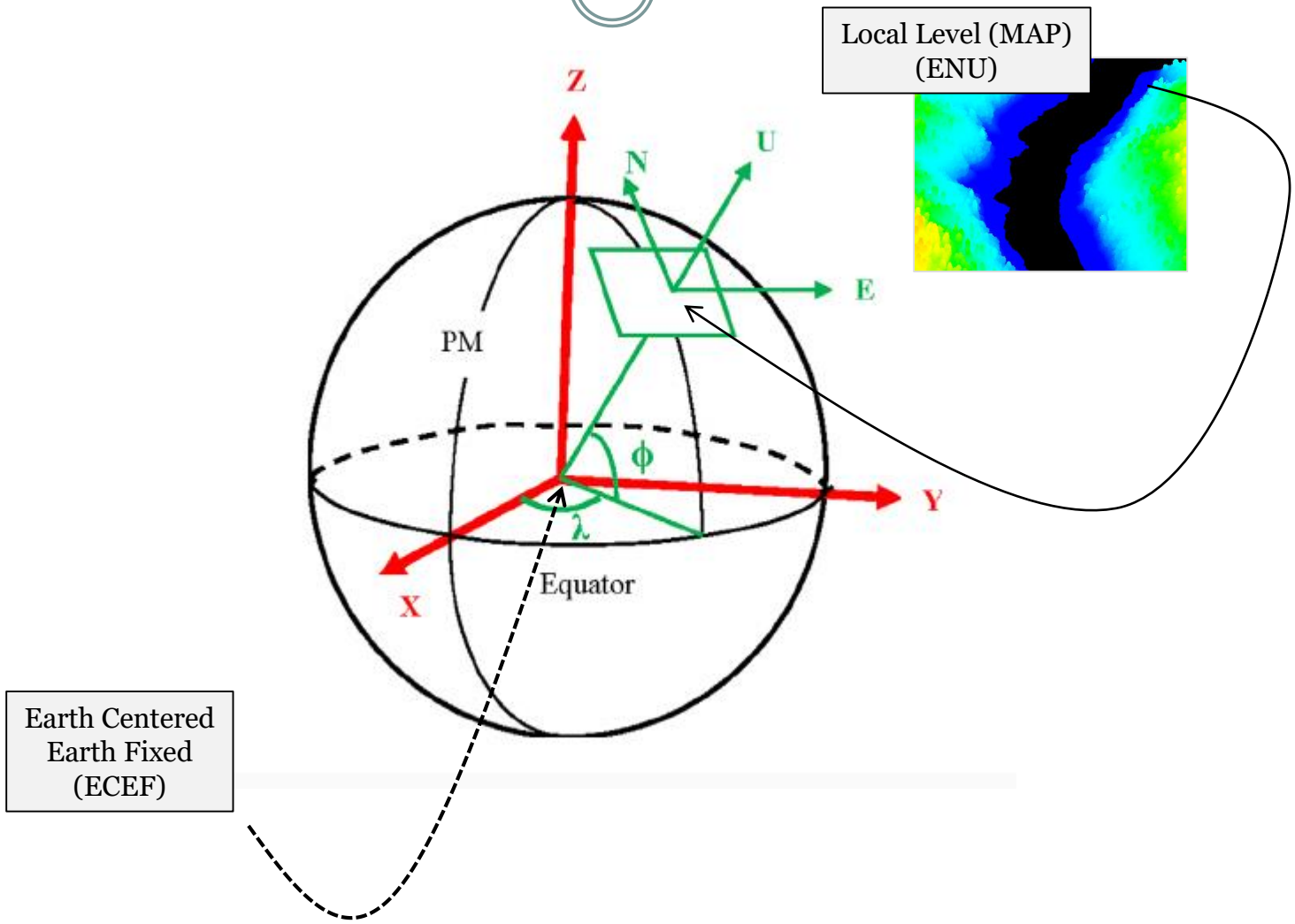

Local Level (Map) to ECEF

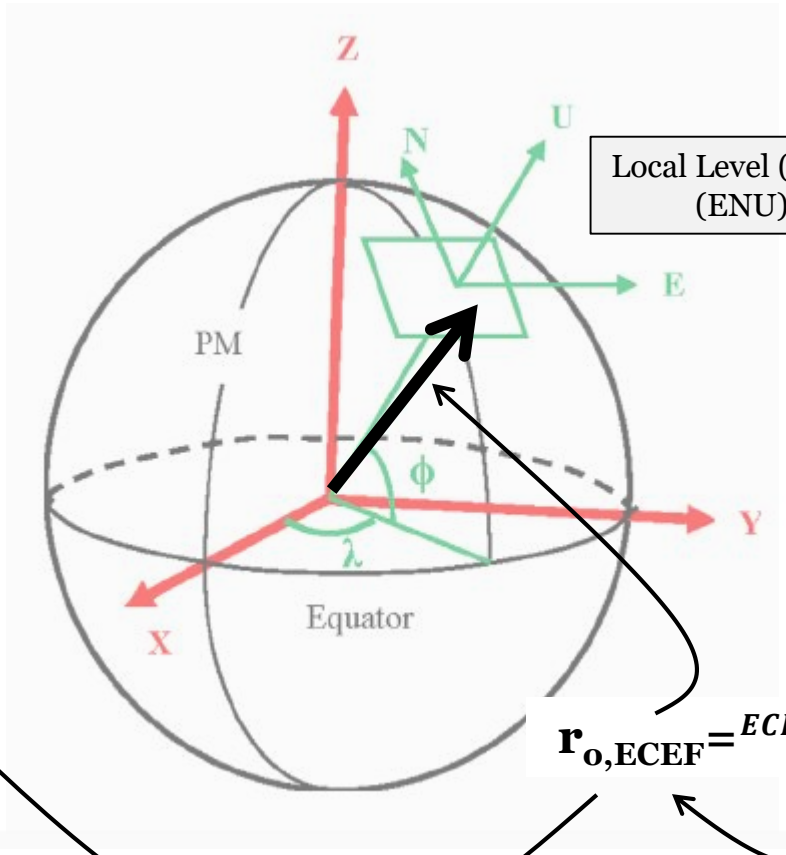

Local Level (MAP)
(ENU)

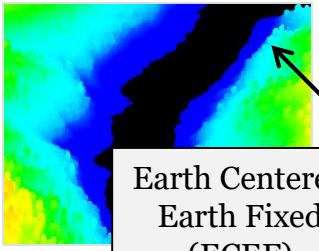

Earth Centered
Earth Fixed
(ECEF)
<x,y,z>

$$\mathbf{r}_{\mathbf{o,ECEF}} = {}^{ECEF}f_M(\mathbf{r}_{\mathbf{o,M}}, \mathbf{r}_{\mathbf{origin,M}})$$

Diagram: Wang, Huynh, Williamson

ECEF to Geodetic (Lat, Lon, Alt)

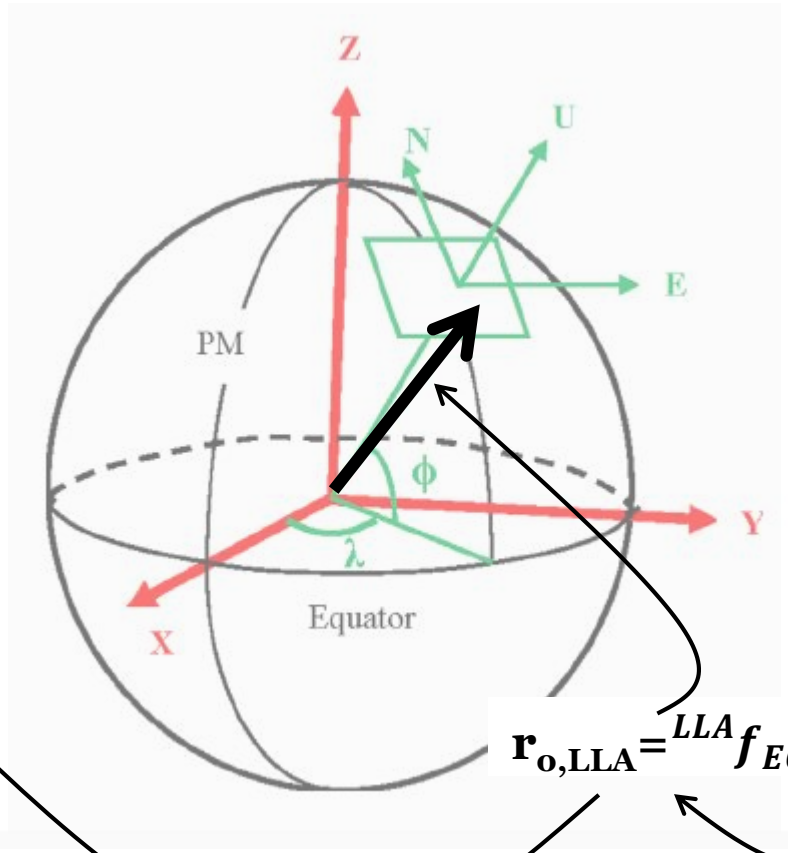

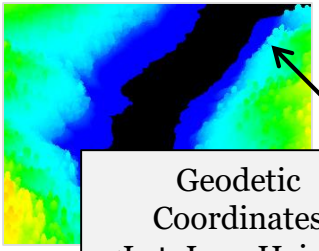

Geodetic
Coordinates
<Lat, Lon, Height>

$$\mathbf{r}_{o,LLA} = {}^{LLA}f_{ECEF}(\mathbf{r}_{o,ECEF}, \mathbf{Datum})$$

Diagram: Wang, Huynh, Williamson

LiDAR data: Georeferenced

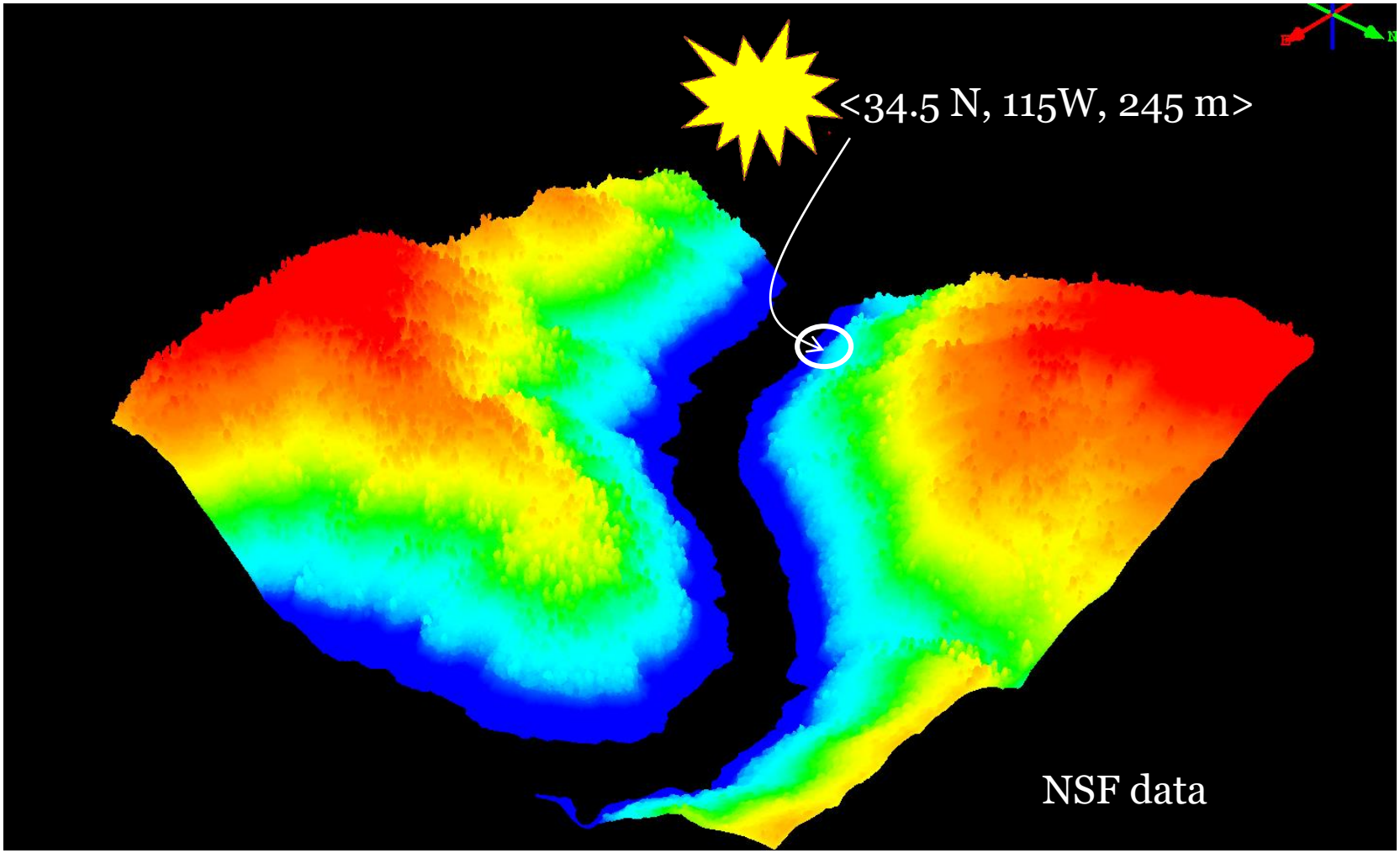

LiDAR Range Extraction and Georeferencing

- Utilizes Estimation and Detection theory
  - Methods of optimal detection
- Wonderful application of
  - Statistics, probability, and linear algebra
- Involves Geodesy
  - Mappings between world referenced coordinate systems

References

1) Airborne Topographic Lidar Manual, Michael Renslow, Editor

2) Elements of Photogrammetry, Wolf and DeWitt

3) Full-wave topographic lidar: State-of-the-art; Clement Mallet and Frederic Bretar, ISPRS Journal of Photogrammetry and Remote Sensing, 64 (2009) 1-16.

4) Empirical Comparison of Full-Waveform Lidar Algorithms: Range Extraction and Discrimination Performance; Photogrammetric Engineering and Remote Sensing; Christopher E. Parrish, Inseong Jeong, Robert Nowak, and R. Smith; August 2011

5) Decomposition of laser altimeter waveforms; M.A. Hofton, J.B. Minster, and J.B. Blair; IEEE Transactions of Geoscience and Remote Sensing, 38(4):1989-1996

6) 3D vegetation mapping using small-footprint full-waveform airborne laser scanners. Available from: https://www.researchgate.net/248978086_fig8_Figure-2-Gaussian-decomposition-of-the-LMS-Q560-waveform-showing-the-recorded-waveform [accessed 19 Mar, 2017]

7) An EM Algorithm for Wavelet-Based Image Restoration; Mario Figueiredo and Robert Novak, IEEE Transactions on Image Processing, Vol 12, No 8, August 2003.

8) Retrieval of the Backscatter Cross-section in Full-Waveform LIDAR data using B-Splines; A. Roncat, G. Bergauer, N. Pfeifer, IAPRS, Vol. XXXVIII, Part 3B, Saint Mande, France, September 1-3, 2010

9) Range determination with waveform recornding laser systems using a Wiener Filter; Boris Jutzi and Uwe Stilla, ISPRS Journal of Photogrammetry & Remote Sensing, 61, 2006, 95-107

10) Gaussian Decomposition and calibration of a novel small-footprint full-waveform digitizing airborne laser scanner; Wolfgang Wagner, Andreas Ullrich, Vesna Ducic, Thomas Melzer, Nick Studnicka, ISPRS Journal of Photogrammetery and Remote Sensing 60 (2006) 100-112.

11) Computer Vision: Models, Learning, and Inference, Simon J.D. Prince, Cambridge University Press